6

# Tunable, Narrow Linewidth, High Repetition Frequency Ce:LiCAF Lasers Pumped by the Fourth Harmonic of a Diode-Pumped Nd:YLF Laser for Ozone DIAL Measurements

Viktor A. Fromzel, Coorg R. Prasad, Karina B. Petrosyan, Yishinn Liaw, Mikhail A. Yakshin, Wenhui Shi, and Russell DeYoung[1]
*Science and Engineering Services, Inc.*
*[1]NASA Langley Research Center*
*USA*

## 1. Introduction

Ozone plays a crucially important role in all aspects of human life, although it is only a trace gas present in the middle and low atmosphere. Variations in ozone concentration in the stratosphere have an affect on the protection of the earth's biosphere from the harmful portion of the Sun's ultraviolet rays. Tropospheric ozone initiates the formation of photochemical smog and in high concentrations is harmful to human health and vegetation. Also ozone has a significant influence on the earth radiation budget. Human activities have produced adverse effects on atmospheric ozone distribution, which it left unchecked could lead to catastrophic changes to the biosphere . Hence the continuous measurement of ozone with good spatial resolution over large regions of the globe is an important scientific goal. A remote sensing technique for the monitoring of ozone concentration based on differential absorption lidar (DIAL) has been established as a method providing rapid and precise time and spatial resolutions [Browell, 1989, Richter, 1997]. Ozone absorbs strongly in the UV over the 240 – 340 nm region and also in the IR at near 9.6 μm. A two-wavelength differential absorption technique in the UV is commonly used for ozone measurement. After obtaining the lidar signals at two neighboring wavelengths (on- and off-line), the differential absorption due to ozone is obtained by taking the ratio of the two signals to eliminate the contribution to extinction from scattering commen to both signales. Since the ozone absorption in UV exhibits a smooth band structure, the separation between the on- and off-line wavelengths is required to be a few nanometers.

A number of ground-based [Profitt & Langford, 1997] and aircraft-based DIAL [Richter et al.,1997] systems for monitoring ozone concentrations in the planetary boundary layer, the free troposphere and the stratosphere have been developed by research groups all over the world [McGee et al, 1995, Mc Dermit et al,1995, Carswell et al,1991, Sunesson, et al,1994]. Most of the ground-based ozone DIAL instruments utilize large excimer gas lasers and Raman wavelength shifters, or flashlamp pumped frequency tripled and quadrupled Nd:YAG lasers and dye lasers, which are large complex systems requiring considerable

Source: Advances in Optical and Photonic Devices, Book edited by: Ki Young Kim,
ISBN 978-953-7619-76-3, pp. 352, January 2010, INTECH, Croatia, downloaded from SCIYO.COM

maintenance. Many different approaches have been used to improve the efficiency and reduce the size and complexity of the UV lasers required, for example, for airborne ozone DIAL systems. These systems consist of multi-stage solid-state laser systems involving Nd:YAG pump lasers, and some combinations of optical parametric oscillators, or Ti:Sapphire lasers and frequency mixers and solid-state Raman frequency shifters [Richter, 1997, Profitt & Langford, 1977]. However, all of them are still large, and/or complex and they present enormous challenges for adapting them to autonomous operation.

In conventional lidar systems, high energy laser pulses (~100 mJ) are utilized to obtain a sufficiently large lidar signal to achieve adequate signal to noise ratio (SNR). A different approach can be used, wherein a much smaller laser energy (~ 1 mJ) is sufficient to achieve good lidar performance. This calls for a much smaller all-solid-state laser system that makes it possible to conform to the playload bay constraints of a small aircraft or other small movable platform. By operating the laser at much higher pulse repetition rate (PRR = 1 kHz), the average transmitted power (1 W) is maintained at the same level as that of the bigger laser (100 mJ, 10 Hz, 1 W), despite the much smaller laser energy output (1 mJ) per pulse. The smaller resulting signal is effectively measured by a low noise photon counting PMT detection system, whose dark noise counts are in the 10 to 100 Hz range, making the detector noise negligible. By averaging the signal over a few seconds it is possible to achieve adequate SNR by reducing the contribution of the signal shot noise to SNR. Overall system size and complexity are reduced by this approach making the system rugged, compact and easy to maintain. The recent advances in compact diode-pumped solid state lasers provide an attractive option for the development of compact and effective laser transmitter for ozone lidar. While the DPSS lasers are suited for providing only moderate pulse energies, they can operate at high pulse repetition rates of several kHz to produce reasonably high average power. It is possible to generate tunable UV output starting with the UV DPSS laser, by two different techniques both of which are now commercially available. The first method involves pumping an OPO with a frequency tripled Nd:YAG (355 nm) to generate continuously tunable output spanning 560 to 630 nm and then frequency doubling it to obtain the required range of 280 to 315 nm. But the efficiency of this system is very low in view of the multiple non-linear conversion steps. The second method is simpler and more efficient, and involves a Ce:LiCAF laser [Stamm, et al, 1997, Govorkov, et al, 1998, Fromzel & Prasad, 2003] pumped by an appropriate commercially available frequency quadrupled diode-pumped Nd laser to provide direct UV tunability.

In this chapter, a new development of all-solid-state Ce:LiCAF tunable UV laser (280nm – 315nm), which utilizes a single step conversion of the pump wavelength in Ce:LiCAF crystal, when pumped by frequency quadrupled diode-pumped Nd:YLF laser is described. This laser is the central component of a very compact ozone DIAL system. With moderate (~1mJ) pulse output but high pulse repetition rate (1 kHz) this laser system has a good performance capability. This laser is a further development of a previously reported Ce:LiCAF laser producing ~ 0.5 mJ pulse output at 1 kHz with a 46% conversion efficiency [Fromzel & Prasad, 2003].

## 2. Requirements to laser transmitter for DIAL ozone measurement

Specific character of ozone absorption line and its distribution in atmosphere as well as necessary accuracy of the ozone DIAL measurements determine requirements to parameters of the laser transmitter (energy, PRF, pulse duration, integration time). To establish this

relationship, we will consider basic factors which have influence on this accuracy. As it was mentioned above, in DIAL measurements the differential resonant absorption $K(\lambda_n)$ - $K(\lambda_f)$ is obtained by taking the ratio of two atmospheric backscattered signals received by the lidar at the on- and off- wavelengths $\lambda_n$ and $\lambda_f$. from range $R$. Ozone concentration is then calculated from the mean differential absorption coefficient $K$ for the range cell layer of thickness $\Delta R$ by using the known ozone differential absorption cross section $\Delta\sigma = (\sigma_n - \sigma_f)$ where $\sigma_n$ and $\sigma_f$ are absorption cross sections at the on- and off-line wavelengths. A number of papers have analyzed the sensitivity and accuracy of the DIAL technique [Ismail & Browell, 1989, Korb et al, 1995]. The accuracy of the ozone concentration $n_{O3}$ measurement is calculated by using the relation [Grant, et al, 1991]:

$$\frac{\Delta n_{O3}}{n_{O3}} = \frac{1}{n_{O3}\ \ 2\Delta\sigma\ \ \Delta R\ \ N_s^{1/2}\ (SNR)} \tag{1}$$

here $N_s$ is the number of laser shots, and $SNR$ is the signal to noise ratio of the DIAL measurement which includes the SNR of both the on-line and off line signals. The accuracy of the measurement is thus improved by: averaging over larger number shots, increasing the range cell size, increasing the differential absorption and increasing the signal to noise ratio of the measurement. The parameters which determine the range are: the ozone differential absorption cross section; the distribution of ozone along the path at the time of the measurement; other sources of extinction, such as aerosol loading, fog, etc; the choice of the on- and off-line wavelengths for ozone. From equation (1), it is seen that the accuracy and the range resolution can be improved by choosing the wavelengths so as to provide a large differential absorption cross section (i.e., a large $\Delta\sigma$). However this also makes the differential scattering cross section: $\Delta\alpha = \alpha(\lambda_n) - \alpha(\lambda_f)$ large. Correcting for this requires knowledge of the molecular and aerosol distributions also. Furthermore, the signal strength depends on the atmospheric extinction. Hence the choice of optimal wavelength depends on a number of parameters, which include: the required range, range resolution, temporal resolution (i.e., measurement time), measurement accuracy, and the expected spatial distribution of ozone in the atmosphere.

Figure 1 shows the ozone absorption spectrum between 240 and 340 nm. Below 300 nm, absorption is dominated by the Hartley continuum superimposed by weak Hartley bands. Band structures seen at wavelengths longer than 300 nm are the Huggins bands. While the strongest absorption occurs at 260 nm these wavelengths will be completely attenuated after traveling a short distance and are therefore unsuitable for achieving significant range. Conversely, wavelengths longer than 300 nm are able to penetrate into the high ozone concentrations that are characteristic of the stratosphere, but give small differential absorption signals at the typical tropospheric ozone concentrations. Further, since the absorption cross sections in the Huggins bands also vary significantly with temperature, this region of the spectrum is not very useful for tropospheric measurements where the temperature is highly variable.

Thus, the optimal wavelength range for tunable ozone laser transmitter depends on atmospheric region of interest setting in the UV spectrum between 280 and 300 nm. Comparison of calculated ozone lidar performance for two types of UV lasers operating in the required wavelength region with different characteristics: laser with low energy but high PRF (1 mJ/pulse, 1kHz) and photon counting for detection and laser with high energy but low PRF (100 mJ, 10 Hz) and conventional analog detection shows that the low energy

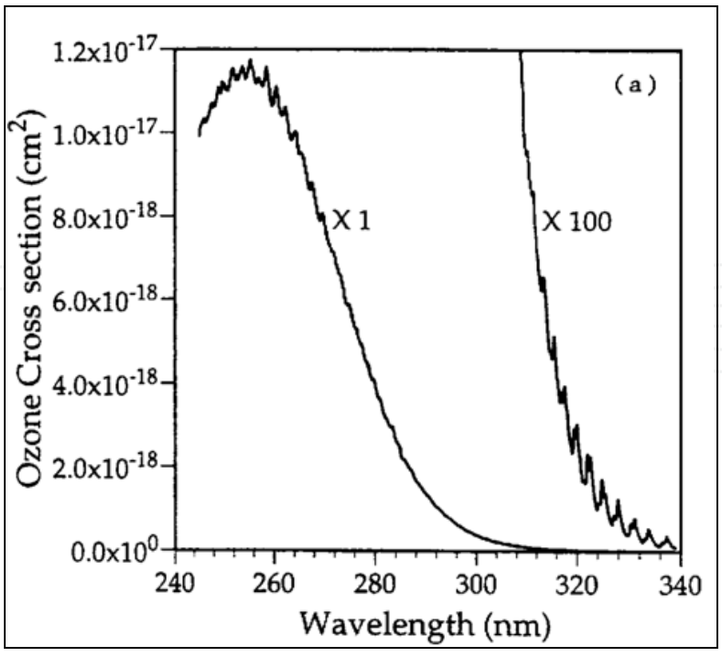


Fig. 1. Ozone absorption spectrum in UV.

laser gives a much higher SNR for all cases of lidar operation. The feasibility of such approach for ozone DIAL - using a low energy, high PRF laser along with photon counting detection have been also demonstrated experimentally [Prasad, et al, 1999]. The Ce:LiCAF laser, which is the best suited for modest energy outputs in the range of 1 to 10 mJ/pulse, presents a very effective direct method of generating the required wavelengths. The principal reasons for this are:

1. Laser linewidths of the order of 0.2 nm are adequate for ozone DIAL. Hence a fairly simple Ce:LiCAF laser system can be designed with a single intra-cavity prism for generating tunable wavelength with the necessary linewidth, with no need for highly selective dispersive elements.
2. The spectral bandwidth of the pump laser does not have to be narrow, because of the broad absorption spectrum of Ce:LiCAF material.
3. Directly tunable laser allows rapid change of wavelength, as it required in hopping from on- to off-wavelengths.

## 3. Spectroscopic and thermo-mechanical characteristics of Ce:LiCAF crystals

Cerium doped crystals Ce:$LiCaAlF_6$ and Ce:$LiSrAlF_6$ (Ce:LiCAF and Ce:LiSAF) are well established as efficient laser media, which can operate directly in the UV region. Both Ce:LiCAF and Ce:LiSAF crystals demonstrated good conversion efficiency (up to 46%) when pumped by the fourth harmonic of Nd:YAG or Nd:YLF laser (266 or 262 nm). Figure 2 shows the spectral absorption and fluorescence of Ce3+ in LiCAF and LiSAF. Their strong absorption at 266 nm (~ 7.5 x $10^{-18}$ $cm^2$ for π-polarization), broad emission spectrum (280 – 325 nm), high emission cross-section (~ 6.8 x $10^{-18}$ $cm^2$ for Ce:LiCAF at 290 nm for π-polarization), and broad tunability (280 -328 nm) make them well suited for ozone DIAL

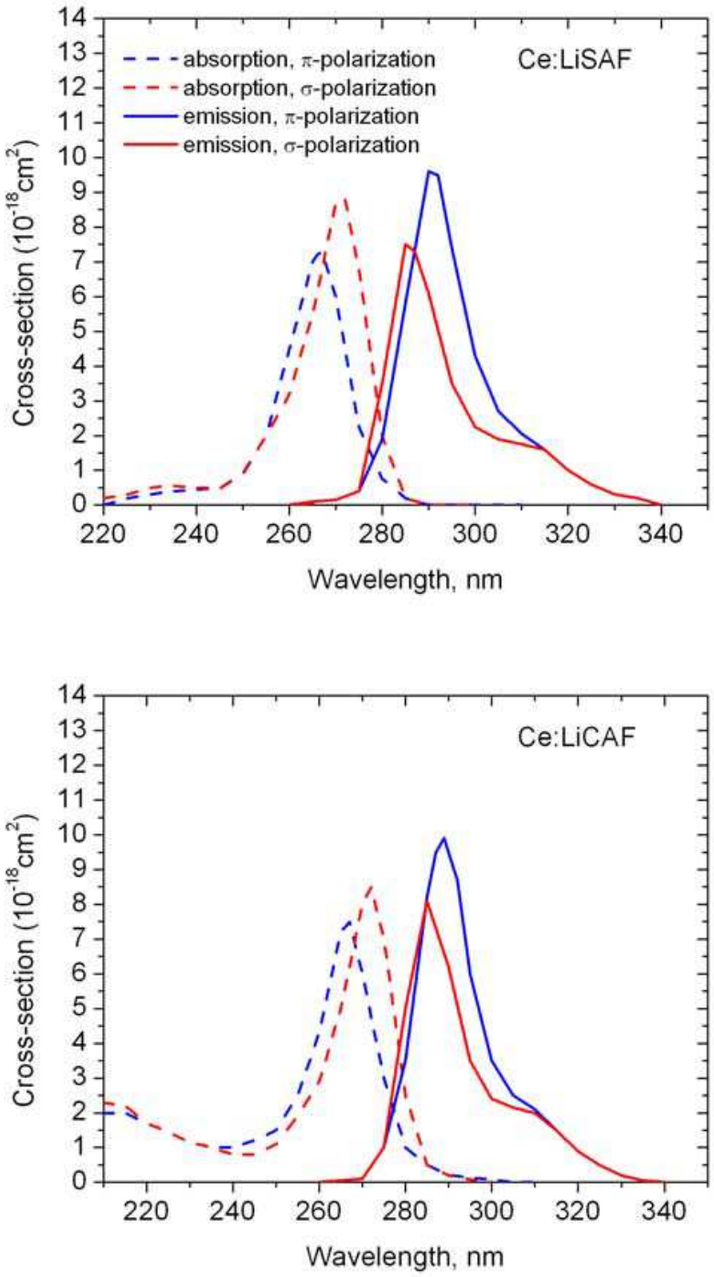


Fig. 2. Polarized absorption and emission spectra of Ce:LiSAF and Ce:LiCAF (π-parallel and σ-perpendicular to the optical axis)

application. Since the cross-section for absorption at 266 and 262 nm are fairly high, the Ce3+ dopant concentration of a few percent (1 – 4%) is enough for complete absorption of the pump. Of the two, Ce:LiCAF is better suited for the high PRF operation, because its spectroscopic properties are slightly better, it is more mechanically robust, and has much better solarization properties for withstanding high power pumping at 266 or 262 nm than

that of Ce:LiSAF. The fluorescence lifetime both Ce:LiCAF and Ce:LiSAF crystals are short (27 and 25 ns, respectively). This implies that the nanosecond pulse durations are required for pumping of Ce:LiCAF (or Ce:LiSAF) lasers and the laser output is gain-switched by the pump laser pulse. Also it means that a short resonator is preferred for the Ce:LiCAF laser.
The thermal conductivity of both LiCAF and LiSAF are low and anisotropic in nature (5.14 - 4.58 and 3.09 - 2.9 W/m$^{o}$C, respectively). Thus even for the low thermal loading (~ 1 W), a noticeable temperature gradient is set up within the crystal. Considering a 3.5% Ce:LiCAF crystal of 8 x 3 x 10 mm (thickness 3 mm), the calculated temperature rise in the crystal will be as $\Delta T \sim 17^{0}$C.

## 4. Diode-pumped frequency quadrupled Nd:YLF laser

From our previous experience with designing of a tunable Ce:LiCAF laser producing 0.5 mJ pulse energy at 1 kHz PRF, it was estimated that in order to obtain ~1 mJ/pulse UV tunable output from Ce:LiCAF laser the pump Nd:YAG or Nd:YLF laser has to provide pulse energy in excess of ~ 11 - 12 mJ in a $TEM_{00}$ beam profile at the second harmonic (532 or 527 nm) that will allow to have ~ 2.8 -3.0 mJ/pulse at the forth harmonic (266 or 263 nm). Such $TEM_{00}$-mode green laser was developed by Positive Light company on the base of the commercial multomode Nd:YLF Evolution 30 laser and supplemented by us with the fourth harmonic module (263 nm).
The optical layout of the Nd:YLF laser with the intracavity frequency doubling (Evolution – $TEM_{00}$) is shown in Figure 3. It consists of a Nd:YLF laser rod that is side-pumped by laser diode arrays. Two high reflective end mirrors M1 and M2 (HR @ 1053nm) form the Nd:YLF laser resonator. The resonator includes a reflective telescope (mirrors TM1 and TM2) that serves to increase the beam size incident on the Nd:YLF crystal. The laser beam is then intracavity frequency doubled by a non-critically phase matched LBO crystal and delivers an output green beam (527nm) through the harmonics separating mirror, which is highly transparent at 527 nm and highly reflecting at 1053nm. An acousto-optical Q-switch performs Q-switched laser operation at 1 kHz repetition rate. The LBO doubling crystal is placed in a temperature regulated oven (154$^{o}$C) to achieve the non-critical phase matching conditions. Figure 4 shows the 527 nm output performance for the frequency doubled diode-pumped Nd:YLF laser, while Figures 5 shows a temporal pulse profile of the Evolution $TEM_{00}$ laser. It may be noted that the pulse duration is very long and with a half width (FWHM) slightly smaller than 100 ns, when diode pump current is 24 Amp (close to

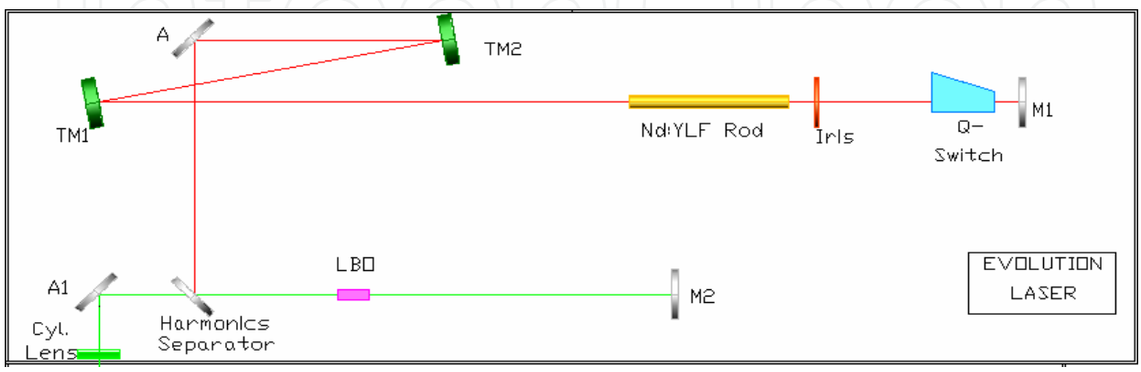


Fig. 3. Optical schematic of the intra-cavity frequency doubled diode pumped Nd:YLF $TEM_{00}$ pump laser.

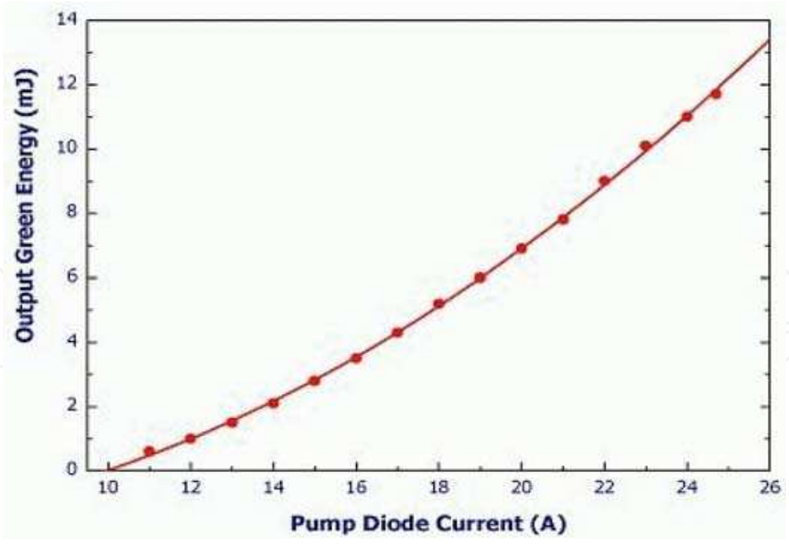


Fig. 4. Intracavity doubled green (527 nm) output of diode pumped Nd:YLF laser.

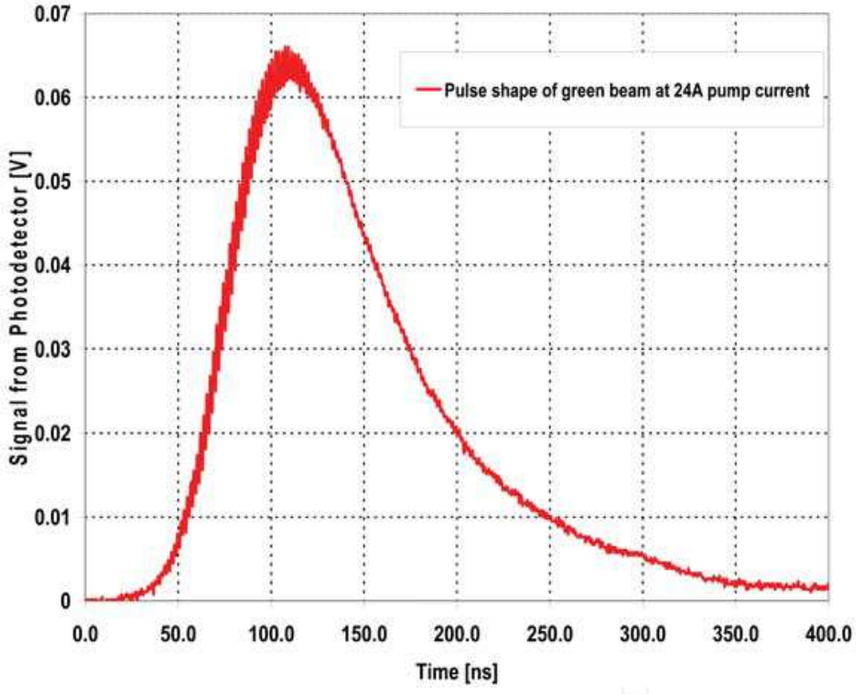


Fig. 5. Temporal profile of the green (527 nm) output pulse of the pump Nd:YLF laser

the maximum of pump current). This long pulse duration is caused by a large length of the laser resonator (~2 m) and also by the fact that the output coupling of resonator is not optimal, because the only load for the resonator is the second harmonic generation. Measurement of spatial profile of the green beam showed that the output beam being very close to the $TEM_{00}$ mode ($M^2$ ~ 1.5) at the same time exhibited a significant amount of astigmatism, with the beam divergence being about 1 x 1.5 mrad in the X and Y directions, respectively. The second harmonic output beam (527 nm) measured at the output window of the laser was slightly elliptic with a diameter of about 0.9 x 1.1 mm for an output of 12 mJ.

The second step in building of appropriate UV pump laser for Ce:LiCAF was development of an efficient CLBO fourth harmonic generator for a 1 kHz, diode-pumped Nd:YLF laser. CLBO is well established as the nonlinear material of choice [Mori, et al, 1995] for efficient fourth harmonic conversion of diode-pumped solid-state neodymium lasers with moderate pulse energies but high average powers and high PRF. CLBO has a high nonlinear coefficient and a large temperature and angular acceptance. However, CLBO is highly hygroscopic [Taguchi, et al, 1997] in nature and thus any exposure of the crystal to humid (>20%) atmospheric conditions causes rapid degradation of the crystal surface, which can lead to a reduced performance and/or optical damage. A simple technique to avoid the problems associated with CLBO crystal is to maintain the crystal at >150$^{o}$C, so that atmospheric humidity does not degrade the crystal. To avoid the crystal degradation, a special crystal ceramic oven for maintaining the crystal temperature at temperature of ~152$^{o}$C has been constructed and was heated all the time being supplied from a battery backed UPS power source.t should be noted that the Evolution $TEM_{00}$ laser output was no optimum for obtaining the best fourth harmonic conversion efficiencies because its pulse duration was fairly long (~ 100 ns) and the beam was not true $TEM_{00}$-mode showing some astigmatism: different beam divergences in the x- and y-directions. In spite of the non-optimal 527 nm beam, a fairly high fourth harmonic conversion efficiency (~ 25%) have been achieved in the 15 mm long uncoated CLBO crystal by using mode matching optics. At this output, the mean incident energy density on the CLBO crystal was ~ 25% lower than the damage threshold and the CLBO crystal was operated in a safe damage free regime. Figure 6 shows the fourth harmonic energy output as a function of the diode pump current for the Nd:YLF laser. At maximum diode current of the Nd:YLF laser of 25 A, the fourth harmonic output was as high as 2.85 mJ/pulse.

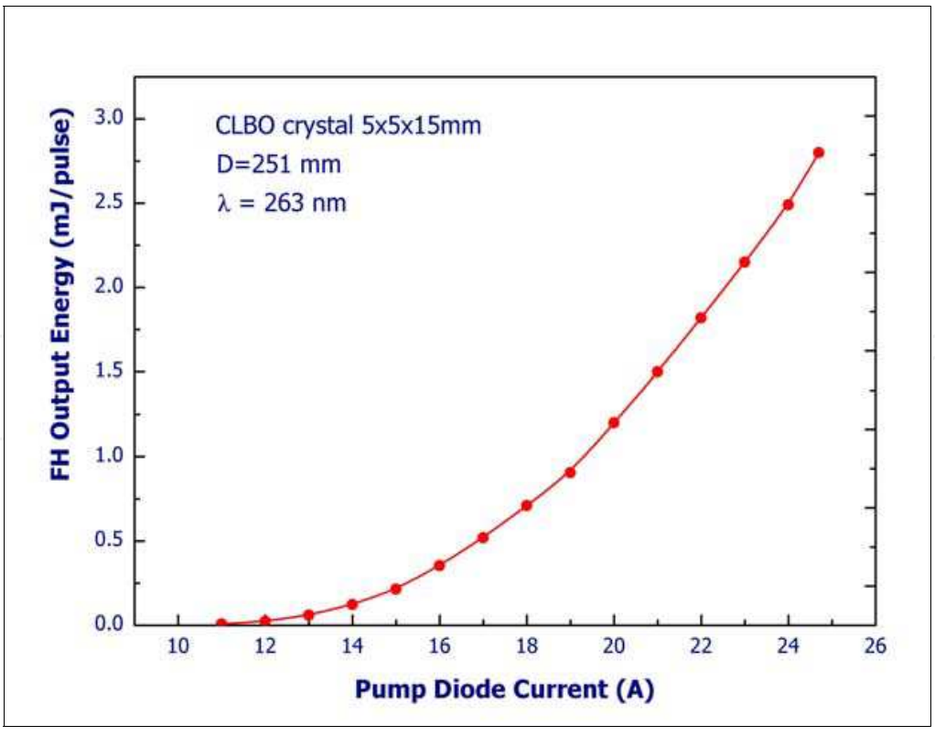


Fig. 6. Output from the optimized CLBO fourth harmonic generator shown as a function of the diode current for pump green laser.

## 5. Ce:LiCAF tunable UV laser

The optical schematic of the Ce:LiCAF laser is shown in Figure 7. A pair of $CaF_2$ rectangular prisms was used for separation of the second and fourth harmonic pump beams and for beam folding. After that the incoming 263 nm UV pump beam was split by a fused silica beam splitter (40% and 60%) into two parts and directed to the Ce:LiCAF crystal faces by four 100% reflecting folding mirrors. The pumped spot size on the Ce:LiCAF crystal has an elliptical shape with dimensions of ~ 0.4 x 0.65 mm. Pump spot sizes on the Ce:LiCAF crystal were chosen carefully to avoid optical damage of the crystal, to obtain good conversion efficiency and to provide $TEM_{00}$ operation of Ce:LiCAF laser. A Brewster cut 3.5% doped Ce:LiCAF crystal with dimensions of 2 mm (thickness) x 8 mm (width) x 10 mm (length) is pumped from both faces. The measured absorption of this crystal at 263 nm (π-polarization) was found to be $k_{263}$ = 4.47 $cm^{-1}$, and ~ 98% of the incident pump power is absorbed in the crystal. The Ce:LiCAF crystal is mounted on a copper crystal holder heat sink which is maintained at about 20°C. The Ce:LiCAF laser resonator consists of a flat mirror (HR @ 280-320 nm) and a curved output coupler ( $R_{out}$ = 0.6 @ 280-320 nm, RoC = 1 m) with an intra cavity fused silica (suprasil) prism as a wavelength selector which results in a linewidth of 0.15 – 0.2 nm. The pumping beams are focused into the Ce:LiCAF crystal by means of two fused silica lenses (200 mm focal length). The tilt angle between the pump beams and the Ce:LiCAF laser beam is ~ 2.5°. Wavelength tuning of the laser is performed by rotation of the flat HR mirror of the resonator in horizontal plane. Because direction of the beam between output coupler and Ce:LiCAF crystal stays unchangeable, such tunable laser resonator design provides output beam pointing stability and collinearity better than +/- 0.05 mrad whereas wavelength of the laser is tuned. The length of the resonator is ~ 12 cm. A slightly off-axis pumping scheme is used here. This configuration provides a significant advantage by spatially separating the pump and laser beams so that the pump beam does not have to pass through the laser mirrors or other optical components of the laser thus avoiding a common problem of optical damage caused by the pump beam.

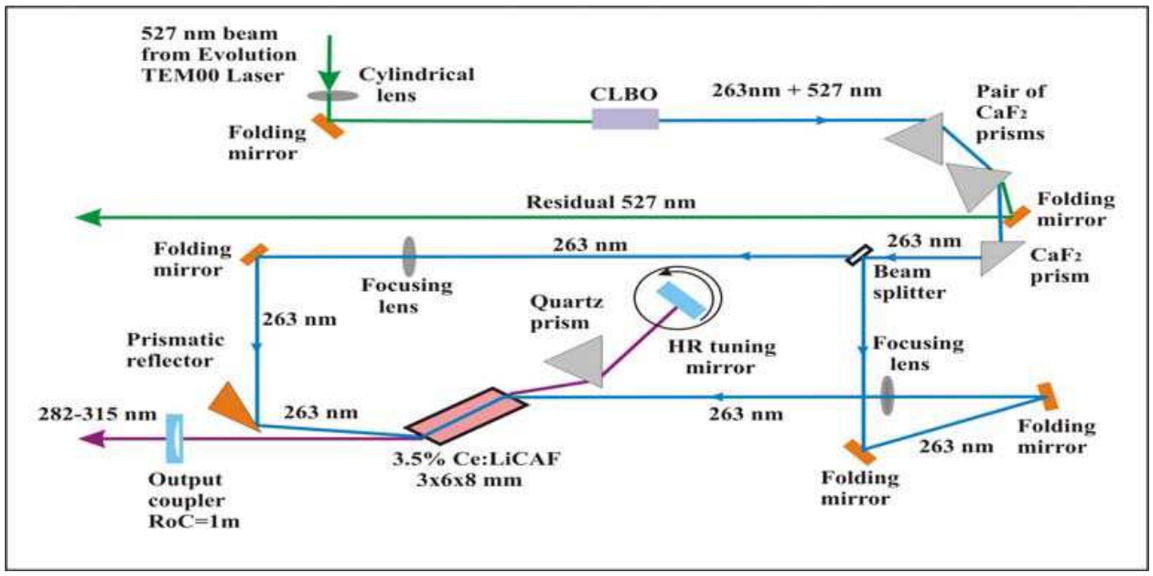


Fig. 8. Optical layout for the double-side pumped Ce:LiCAF laser.

## 6. Ce:LiCAF laser performance

Figure 9 shows the input - output performance of the Ce:LiCAF laser at wavelength of 290 nm with narrow wavelength bandwidth of ~ 0.15 nm when it is pumped by the FH laser beam at 263 nm with a pulse repetition rate of 1 kHz. Output pulse energy 1 mJ/pulse was obtained from the Ce:LiCAF laser when the total incident pump pulse energy on both faces of the laser crystal was 2.86 mJ/pulse. In our experiments, the slope efficiency is ~ 45%, which was found to be about 90% of the theoretical maximum value for the laser [Fromzel & Prasad, 2003]. This result shows that there is nearly full utilization of the pump energy.

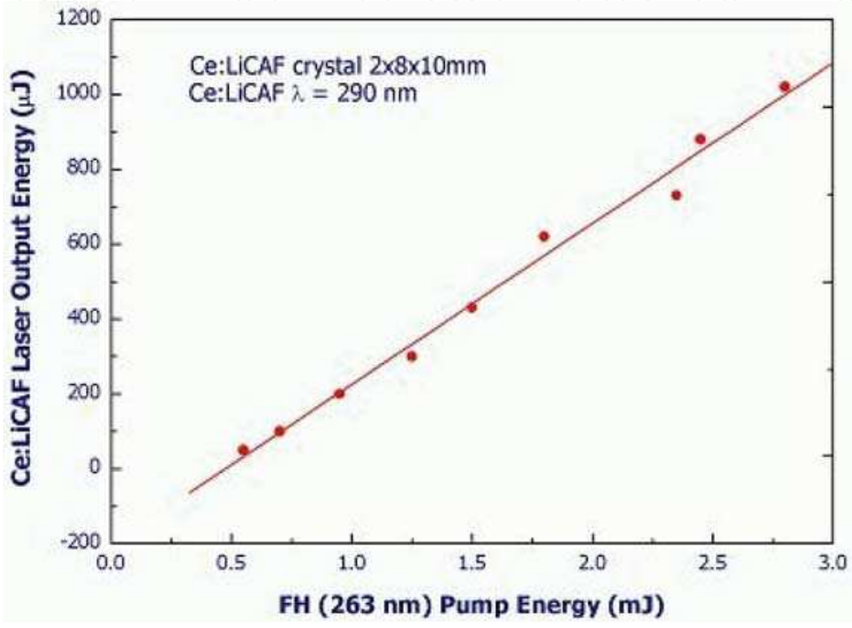


Fig. 9. Input-output performance of the Ce:LiCAF laser pumped from two sides by the fourth harmonic of Nd:YLF laser.

Figure 10 shows the typical temporal shape of the Ce:LiCAF laser pulse. The upper trace is the shape of the pump pulse at 263 nm and the lower trace is the corresponding Ce:LiCAF output pulse. It is noted that in spite of a short pulse duration, typical for Q-switched lasers, the Ce:LiCAF laser operates to the point at free running (gain-switch) regime. It can be clear seen from the fact that the Ce:LiCAF laser output pulse exhibits typical for free running laser operation transient behavior (relaxation oscillations). Thus the pulse length of Ce:LiCAF depends on the pump pulse length. Also shown is the pump laser pulse, and by comparing the two, the build up time for the Ce:LiCAF pulse is seen to be about 48 ns.

The transverse beam shape of the Ce:LiCAF laser output was measured with a beam profiler. It was found that the output laser beam has a true $TEM_{00}$-mode distribution ($M^2$ ~ 1.1) and the profiles are smooth without any hot spots.

Ability of Ce:LiCAF laser to be directly wavelength tuning is one of the advantages of this UV laser, which allows rapid change of wavelength, as it required in hopping from on- to off-line wavelengths, or for sensing ozone at different altitudes. The output wavelength of Ce:LiCAF laser was tuned by rotating the HR tuning mirror which was mounted on a rotary mirror mount. The laser wavelength and linewidth were determined by the intra-cavity dispersing prism. Figure 11 shows a sample laser tuning curve, which was obtained by

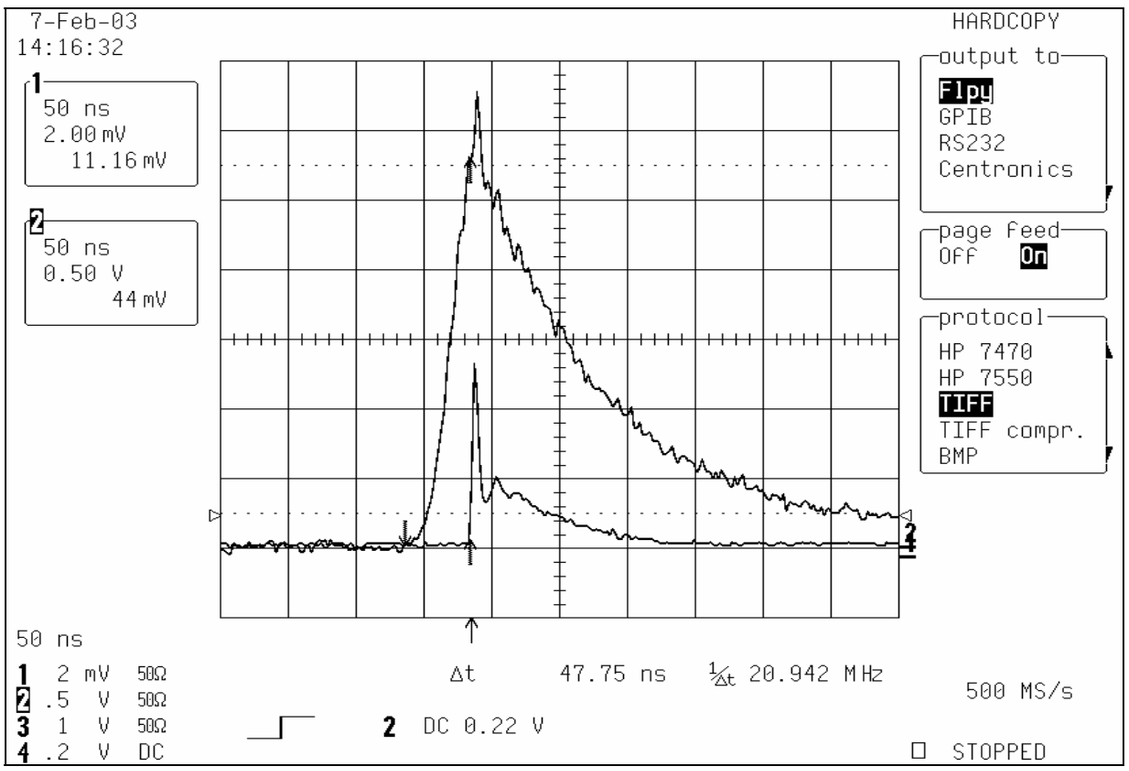


Fig. 10. Shape of the pump UV pulse (upper trace) and the Ce:LiCAF laser output pulse (lower trace).

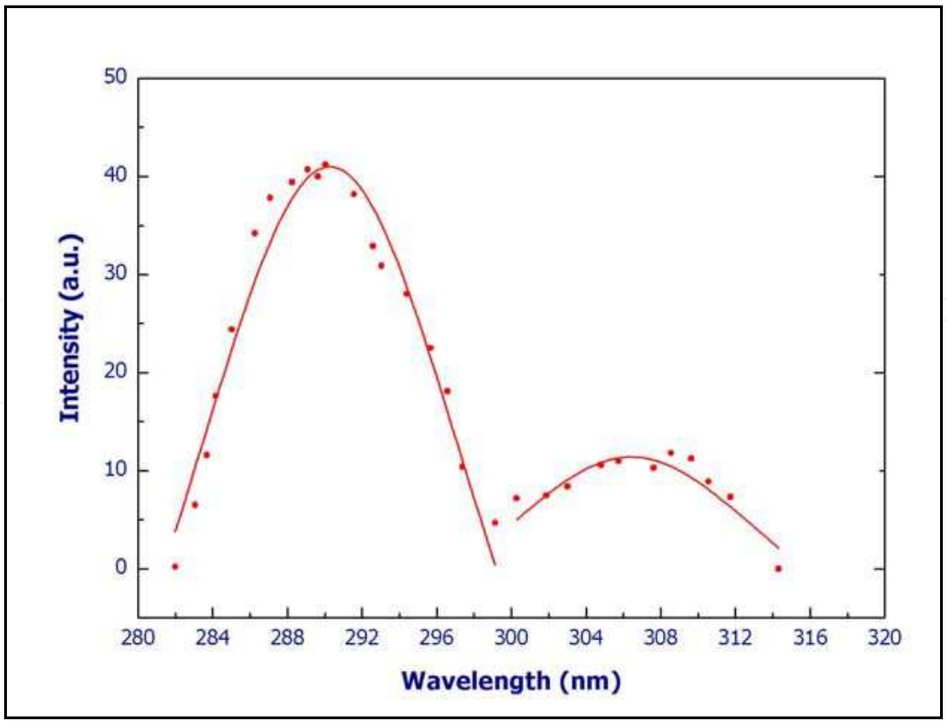


Fig. 11. Tuning curve of the Ce:LiCAF laser.

tuning over a broad spectral region from 281 nm to 316 nm while the 263 nm pump energy was ~ 2 mJ/pulse. Laser linewidth as measured with the Ocean Optics grating spectrometer with a resolution of 0.065 nm was approximately 0.15 – 0.2 nm, when a fused silica dispersing prism was used. The maximum laser output occurred at a wavelength of ~ 290 nm, the second much more weak maximum of laser output corresponded to ~ 308 nm. By using a different prism material with a larger dispersion, such as, sapphire the linewidth can be reduced. With a sapphire dispersion prism the linewidth was reduced to ~0.1 nm. The angular motion required for tuning over 10 nm is approximately 0.3□ for fused quartz and about 0.6□ for sapphire.

It can be concluded from Figure 11 that output pulse energy of the Ce:LiCAF laser reduces approximately four times regarding the maximum of 1 mJ/pulse output at ~ 290 nm, when laser wavelength is tuned to ~ 284 nm or to ~ 297 nm on the short- and long-wavelength edge of the tuning curve, respectively.

## 7. High speed wavelength tuning of Ce:LiCAF laser

Ce:LiCAF laser using as a transmitter for lidar has to supply lidar with both the on- and off-line wavelengths. As it was shown above, wavelength tuning of Ce:LiCAF laser was achieved by changing the angle of the rear mirror. A rapid tuning of the laser output wavelength from shot to shot at pulse repetition frequency of 1 kHz was achieved by mounting the HR mirror on a servo-controlled high speed galvanometric deflector. The tuner control system has been designed to provide pairs of pre-selected "on" and "off-line" wavelengths λ1 and λ2 at 1 kHz operation chosen for ozone differential absorption measurements. It is essential for the "on" and "off-line" wavelengths to be stable both in the short term (i.e., from shot-to-shot) and in the long term (over a period of a few hours). Mechanical backlash, hysterisis, thermal drift and other instabilities affect the short and long term wavelength stability. By utilizing sinusoidal small angle rotations we have eliminated the potential problems of hysterisis and backlash. Long-term drifts are corrected by the feedback control loop embedded into the servo motor drive circuit.The servo controlled mirror is continuously oscillated at 500 Hz to generate harmonic angular deflection as shown in Figure 12. By taking different time delay between the pump laser pulse and the clock, which generates the harmonic drive signal for varying the mirror position, different output wavelengths are produced on every pulse. Then by firing the pump laser with

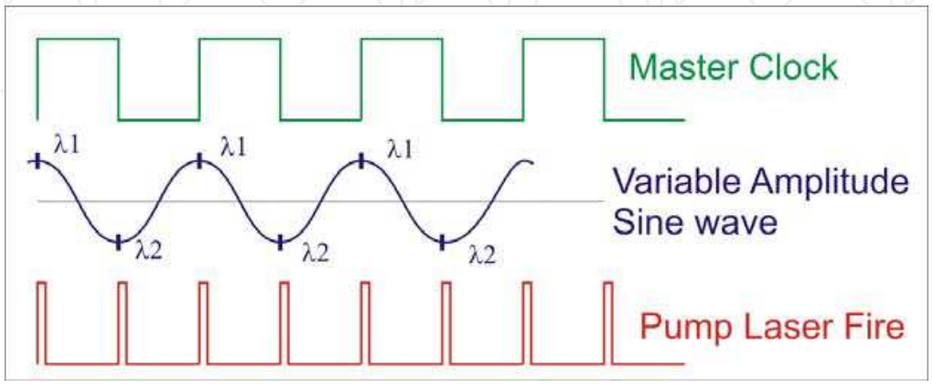


Fig. 12. Basic principle of the high speed tuner for generating pairs of "on-" and "off-"line adjustable wavelengths at 1 kHz PRF.

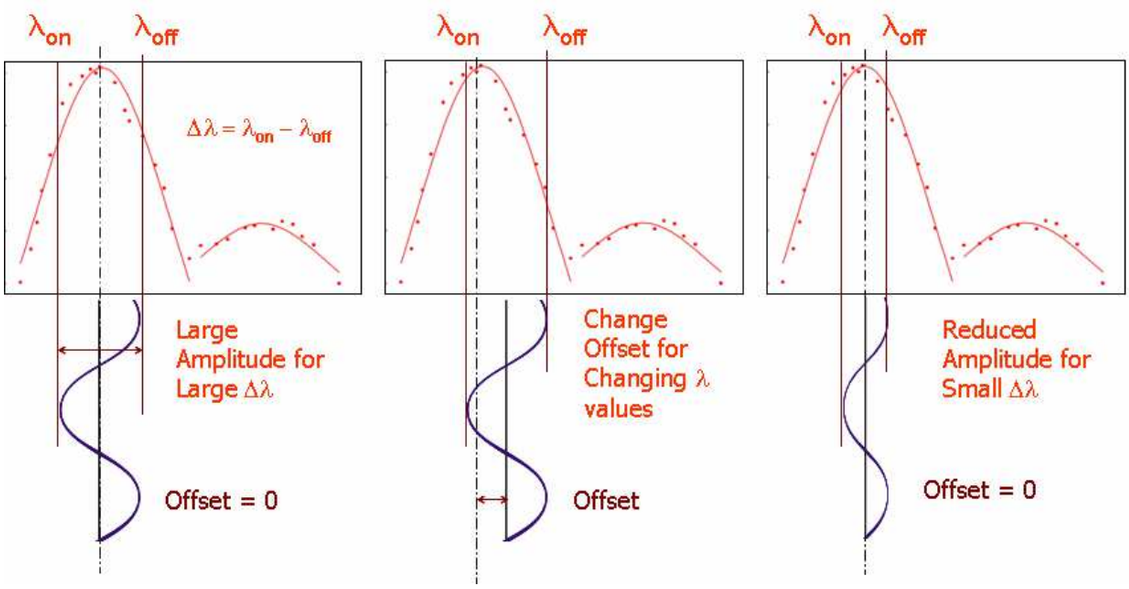


Fig. 13. Amplitude and offset of the harmonic motion of tuning mirror used to select "on" and "off" wavelength

proper time delays on both halves of the harmonic wave, pairs of wavelengths, i.e. an "on-line" and "off-line" wavelength on alternate pulses, are generated when the laser is operated at 1 kHz (see Figure 12). Since a stable master clock is used to synchronize the sine wave, the delays and the laser fire, the pulse variability and jitter are very small (<5ns). Variation of sine wave amplitude determined separation between pre-selected pair of on - and off-line wavelengths of Ce:LiCAF laser, while the offset change moved the pair along the tuning curve of the Ce:LiCAF laser, as it is shown in Figure 13.

## 8. Assembled Ce:LiCAF laser module

All the optical components required for generating the tunable UV output, including the FH generator are housed in a single modular assembly. A mono-block laser head machined from an annealed aluminum block provides a sealed enclosure. Many of the optical mounts were custom designed to achieve adequate rigidity and robustness needed for an airborne laser system. All the optical mounts and fixtures are also constructed out of aluminum to maintain an athermal optical alignment over a wide range of temperatures. Figure 14 shows the component layout of the tunable laser. The Ce:LiCAF crystal is mounted on water cooled heat sink, and the entire assembly sits on a motorized translation stage allowing for repositioning the Ce:LiCAF crystal. If any degradation of the crystal is observed due to solarization, the crystal can be remotely moved by the translation stage to utilize a fresh region of the crystal. It may be noted that the plumbing used for the water cooled heat sink is hard soldered to prevent the possibility of any water leak within the laser head.

The fourth harmonic beam from the CLBO crystal was passed through a pair of $CaF_2$ prisms, which deflect the beam by $90^o$ and also separate the unused second harmonic beam from the UV beam. The UV beam is deflected by an additional $90^o$ in a second set of prisms, to fold the beam. A 2X beam expander is used to expand the beam to avoid damage in the downstream optical components, which include the beam divider and 100% mirrors.

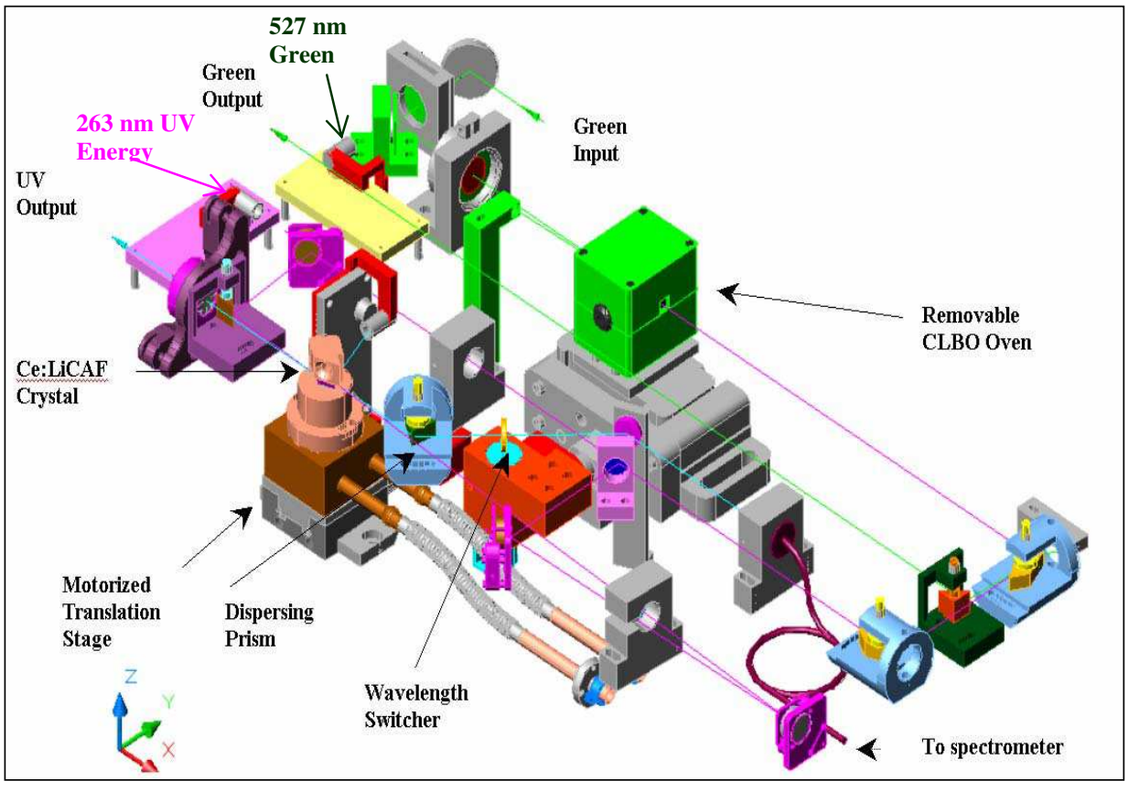


Fig. 14. Component layout of the Ce:LiCAF laser. CLBO crystal is in oven heated to ~ 150°C. CLBO and Ce:LiCAF crystals are placed on motorized mounts.

Figure 15 shows the complete view of tunable laser assembly together with the pump laser. The optical bench is designed such that the water hoses and cables are conveniently accessed from the back of the laser head and there are no cooling lines are inside the head. The main attributes of the laser system are simplicity and ruggedness.

The operation of the Evolution $TEM_{00}$ laser was performed through a computer controlled operator interface residing on PC computer. The same computer was used to operate and control the tunable UV laser.

The central component in the control function is the General Control Unit (GCU) which generates the timing sequence and all the trigger signals required for the wavelength tuning and for the laser operation. It has been implemented using a master clock and a CPLD (128 macro-cell complex programmable logic device). The wavelength controller unit generated the variable amplitude harmonic modulation to dither the galvanometric rotary actuator. A simple interactive computer interface was provided for the operator to choose the values of the required pair of the output wavelengths. During operation the laser output cycles through the chosen wavelengths □1 and □2, sequentially at a 1 kHz pulse repetition frequency.

MS Windows based operator control interfaces have been designed to separately control the Evolution $TEM_{00}$ pump laser, fourth harmonic generator (CLBO crystal) phase match control, and Ce:LiCAF crystal position motors. The pulse energies and temperature at several points in the laser head were monitored with an eight-channel ADC card. The motorized FHG crystal mount stage allowed remote adjustment of the CLBO crystal. Provision was made for feedback control of the stage to achieve optimal phase matched operation.

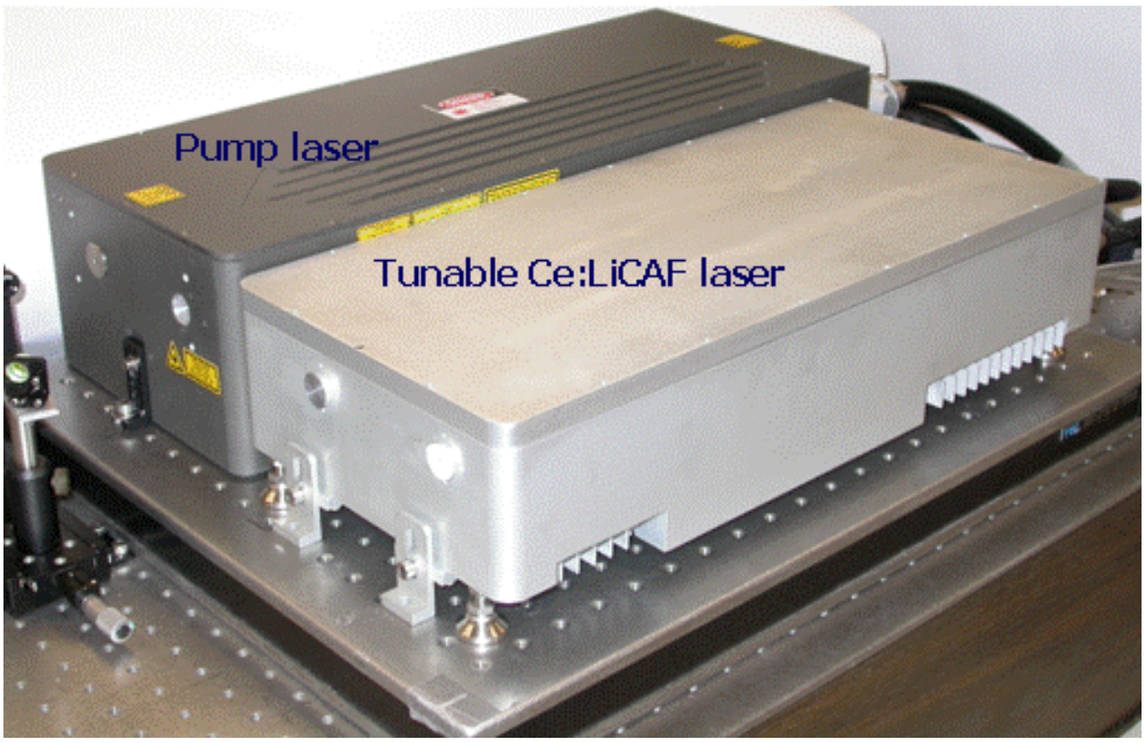


Fig. 15. Complete assembly of tunable UV laser source. The pump laser is the Evolution $TEM_{00}$ (PositiveLight) intra-cavity doubled diode pumped Nd:YLF laser.

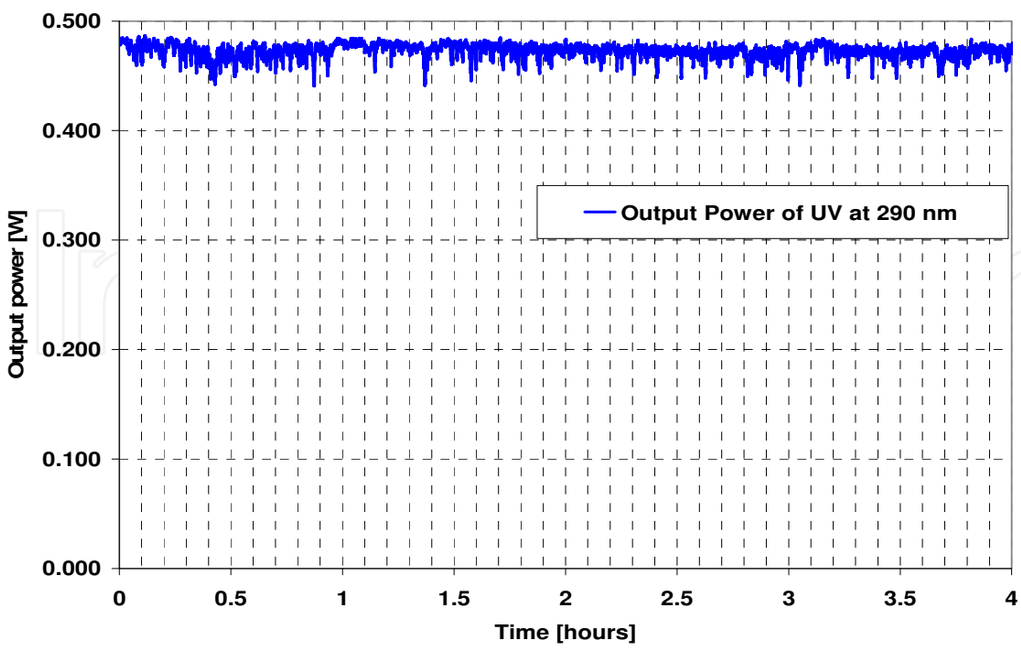


Fig. 16. Daily Long Term stability output power at 290 nm

## 9. Prolonged performance of the Ce:LiCAF laser

In this test, the Ce:LiCAF laser was operating continuously for 4 hours daily during 20 days. The operating conditions were maintained constant over the duration of the test. The output power at the pump wavelengths (527 nm, 262 nm) and of the Ce:LiCaF laser output at 290 nm was continuously monitored. The drift in the phase matching in the CLBO crystal has been periodically revised and eliminated.
The observed variations in Ce:LiCAF output (290 nm) follows those of green pump beam (527nm) and do not exceed 8 %. as showed at the Fig.16.

## 10. Conclusion

A highly efficient, compact and rugged 1 kHz tunable UV Ce:LiCAF laser pumped by the fourth harmonic of a diode–pumped commercial Nd:YLF laser for ozone DIAL measurements has been developed and the performance of this laser was investigated. The Ce:LiCAF laser delivered 1 mJ pulse energy at 290 nm wavelength and was able to be wavelength tuned from 281 to 316 nm that was achieved with a single fused silica dispersion prism in the laser cavity. Fast shot-to-shot wavelength switching was obtained by the harmonic motion of tuning mirror mounted on a servo-controlled high speed galvanometric deflector.

## 11. References

Browell, E.V., (1991). *Differential Adsorption Lidar Sensing of Ozone,* Proc. *IEEE*, 77, pp. 419-432, Carswell.

Fromzel, V.A., and Prasad C.R., (2003). A Tunable Narrow Linewidth 1kHz Ce:LiCAF Laser with 46% Efficiency, *OSA TOPS*, Vol.83, Advanced Solid-State Photonics, pp. 203-209.

Govorkov, S.V.; Weissner, A.O., Schroder, Th., Stamm, U., Zschoke,W., and Basting, D., 1998. "Efficient high average power and narrow spectral linewidth operation of Ce:LiCAF laser at 1 kHz repetition rate," *Advanced Solid State Lasers*, OSA TOPS 19, pp. 2-5.

McGee, T.J.; Gross, M.R., Butler, J.J., and Kimvilakani, P.E., (1995). "Improved stratospheric ozozne lidar", *Optical Engineering*, Vol. 34, pp. 1421-1430.

McDermit, S.; Walsh, T.D., Deslis, A., and White, M.L., (1995). "Optical system design for a stratospheric lidar system," *Applied Optics*, Vol. 34, pp. 6201-6210.

Mori,Y.; Kuroda, I., Nakajima, S., Sasaki, T., and Nakai, S., (1995). "New nonlinear optical crystal: cesium lithium borate," *Appl.Phys. Lett.*, 67, p.1818.

Profitt, M.H., and Langford, A.O., (1977). *Applied Optics*, 36, No.12, pp. 2568-2585,

Richter, D.A., Browell, E.V., Butler,C.F., and Noah,S.H., (1997). *"Advanced airborne UV DIAL system for stratospheric and tropospheric ozone and aerosol measurements"*, Advances in Atmospheric Remote Sensing with Lidar, pp. 317-320, Springer, Berlin.

Stamm, U.; Zschocke, W., Schroder, T., Deutsch, N., and Basting, D., (1997). "High efficiency UV-conversion of a 1 kHz diode-pumped Nd:YAG laser system,"in *Advanced Solid State Lasers*, C.R.Pollock and W.R.Bosenberg, OSA TOPS vol.10, p. 7.

Sunersson, J.A.; Apituley, A., and Swart, D.P.J., (1994). "Differential absorption lidar system for routine monitoring of troposperic ozone," *Applied Optics*, Vol. 33, pp. 7046-705.

Taguchi, A.; Miyamoto, A.,Mori, Y., Haramura, S., Inoue, T., Nishijima, K., Kagebayashi, Y., Sakai, H., Yap, Y.K., and Sasaki, T., (1997). "Effects of moisture on CLBO,"in *Advanced Solid State Lasers*, C.R.Pollock and W.R.Bosenberg, OSA TOPS vol.10, p.19.

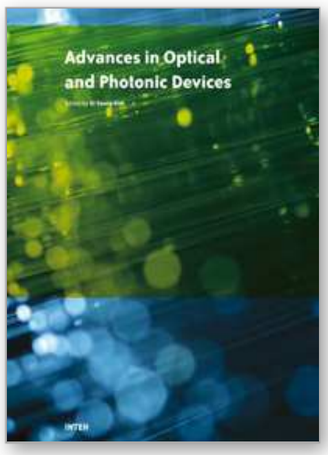


**Advances in Optical and Photonic Devices**

Edited by Ki Young Kim

ISBN 978-953-7619-76-3
Hard cover, 352 pages
**Publisher** InTech
**Published online** 01, January, 2010
**Published in print edition** January, 2010

The title of this book, Advances in Optical and Photonic Devices, encompasses a broad range of theory and applications which are of interest for diverse classes of optical and photonic devices. Unquestionably, recent successful achievements in modern optical communications and multifunctional systems have been accomplished based on composing “building blocks” of a variety of optical and photonic devices. Thus, the grasp of current trends and needs in device technology would be useful for further development of such a range of relative applications. The book is going to be a collection of contemporary researches and developments of various devices and structures in the area of optics and photonics. It is composed of 17 excellent chapters covering fundamental theory, physical operation mechanisms, fabrication and measurement techniques, and application examples. Besides, it contains comprehensive reviews of recent trends and advancements in the field. First six chapters are especially focused on diverse aspects of recent developments of lasers and related technologies, while the later chapters deal with various optical and photonic devices including waveguides, filters, oscillators, isolators, photodiodes, photomultipliers, microcavities, and so on. Although the book is a collected edition of specific technological issues, I strongly believe that the readers can obtain generous and overall ideas and knowledge of the state-of-the-art technologies in optical and photonic devices. Lastly, special words of thanks should go to all the scientists and engineers who have devoted a great deal of time to writing excellent chapters in this book.



INTECH
open science | open minds

**InTech Europe**
University Campus STeP Ri
Slavka Krautzeka 83/A

**InTech China**
Unit 405, Office Block, Hotel Equatorial Shanghai
No.65, Yan An Road (West), Shanghai, 200040, China

www.intechopen.com

51000 Rijeka, Croatia
Phone: +385 (51) 770 447
Fax: +385 (51) 686 166
www.intechopen.com

中国上海市延安西路65号上海国际贵都大饭店办公楼405单元
Phone: +86-21-62489820
Fax: +86-21-62489821



IntechOpen

IntechOpen